


Cite this: *RSC Adv.*, 2022, 12, 3602

# Preparation of biomimetic non-iridescent structural color based on polystyrene–polycafeic acid core–shell nanospheres

Tianchen Wei,<sup>abc</sup> Xiaowei Zhu,<sup>abc</sup> Xueni Hou,<sup>abc</sup> Yijiang Li,<sup>abc</sup> Aoqing Dong,<sup>abc</sup> Xinying Jiang,<sup>abc</sup> Yu Huang,<sup>abc</sup> Xue Dong,<sup>\*abc</sup> Xiangrong Wang,<sup>abc</sup> Guoqiang Chen<sup>id</sup><sup>abc</sup> and Tieling Xing<sup>id</sup><sup>\*abc</sup>

Caffeic acid (CA), as a natural plant-derived polyphenol, has been widely used in surface coating technology in recent years due to its excellent properties. In this work, caffeic acid was introduced into the preparation of photonic band gap materials. By controlling the variables, a reasonable preparation method of polystyrene (PS) @polycafeic (PCA)–Cu(II) core–shell microspheres was achieved: 1 mmol L<sup>−1</sup> cupric chloride anhydrous (CuCl<sub>2</sub>), 3 mmol L<sup>−1</sup> sodium perborate tetrahydrate (NaBO<sub>3</sub>·4H<sub>2</sub>O), 2 mmol L<sup>−1</sup> CA and 2 g L<sup>−1</sup> polystyrene (PS) were reacted at 50 °C for 10 min to prepare PS@PCA–Cu(II) core–shell microspheres through rapid oxidative polymerization of CA coated PS of different particle diameters. The amorphous photonic crystal structure was self-assembled through thermal assisted-gravity sedimentation, resulting in structural color nanomaterials with soft and uniform color, no angle dependence, stable mechanical fastness and excellent UV resistance.

Received 28th November 2021

Accepted 20th January 2022

DOI: 10.1039/d1ra08691j

rsc.li/rsc-advances

## 1 Introduction

The colorful colors in nature can be divided into pigment colors, structural colors and the combination of the two according to their different mechanisms of interaction with light.<sup>1</sup> In recent years, structural color materials composed of photonic crystal structures have attracted widespread attention in the fields of display materials,<sup>2</sup> information transmission<sup>3</sup> and biological monitoring<sup>4</sup> due to their superior optical properties. The electromagnetic field theory is the basis for the conception of photonic crystals. From the perspective of electromagnetic fields, photonic crystals are a new type of artificial optical material with photonic energy bands and band gaps composed of several materials with different refractive indices that are periodically distributed and arranged in space. Some researches<sup>5,6</sup> have shown that the modulation and control of photons by photonic crystals is achieved through the photonic band and band gap structure, and the photonic band gap and defects of photonic crystals are directly related to their optical performance. Therefore, research on the materials that

constitute photonic crystals (photonic band gap materials, PBGM) has become the focus of structural color nanomaterials.

The colloidal particle self-assembly method,<sup>7–9</sup> which uses colloidal microspheres with good monodispersity (such as silica and PS microspheres, *etc.*) as the structural unit to assemble the three-dimensional photonic crystal structure, is the most commonly used method for preparing photonic crystals. This method has the advantages of simple operation, low equipment investment requirements and easy preparation of large-area crystals. With the in-depth study on the synthesis of monodisperse colloidal microspheres, it was found that pure inorganic or polymer colloidal microspheres cannot meet the demand in some applications. For example, in the coloring of textiles, the incoherent scattered light masks the structural color and causes the fabric to turn white.<sup>10</sup> At the same time, the inherent iridescent effect of the photonic crystal structure color material also limits its application in the field of color rendering to a certain extent. Designing and constructing composite nanomaterials with special properties, function and stability based on requirements is a common method to broaden the application of structural colors.

Phenols and polyphenols are widely distributed in plant tissues, which link to diverse biological functions such as chemical defense, pigmentation, structural support and prevention of radiation damage.<sup>11</sup> Compared with synthetic polydopamine (PDA), they have lower cost and excellent usability.<sup>12,13</sup> CA is a natural plant-derived polyphenol, which has broad-spectrum antibacterial, antioxidant, UV resistance and other biological activities and functions.<sup>14,15</sup> In the chemical

<sup>a</sup>College of Textile and Clothing Engineering, Soochow University, Suzhou 215123, China. E-mail: dongxue@suda.edu.cn; xingtieling@suda.edu.cn; Tel: +86-512-6706-1175

<sup>b</sup>Jiangsu Engineering Research Center of Textile Dyeing and Printing for Energy Conservation, Discharge Reduction and Cleaner Production (ERC), Soochow University, Suzhou 215123, China

<sup>c</sup>National Textile and Apparel Council Key Laboratory of Natural Dyes, Soochow University, Suzhou 215123, China



structure of CA, the catechol structure similar to dopamine makes it exhibit strong interfacial forces and can directly adhere to any substrate surface,<sup>16</sup> and has been widely used in surface coating technology in recent years. To solve the problem of the long time and low efficiency of caffeic acid oxidation and deposition, Yang *et al.*<sup>17</sup> used copper sulfate ( $\text{CuSO}_4$ ) as an oxidant and hydrogen peroxide ( $\text{H}_2\text{O}_2$ ) as a trigger to promote the rapid oxidation and deposition of PCA, and obtained a uniform, stable and multifunctional dark brown PCA surface coating. Research shows that bright structural colors can be obtained by assembling polystyrene particles coated with a polydopamine shell and the order of arrangement differs depending on the surface roughness.<sup>18</sup> The PCA colored coating was introduced into the preparation of core-shell structured composite nano-colloidal microspheres. In addition, studies have shown that<sup>19,20</sup>  $\text{NaBO}_3 \cdot 4\text{H}_2\text{O}$  can slowly release  $\text{H}_2\text{O}_2$  after being dissolved in water, which can not only replace  $\text{H}_2\text{O}_2$  for oxidation, but also overcome the shortcomings of poor stability, explosiveness, high toxicity, complex operation, and high cost. Moreover,  $\text{Cu}^{2+}$  could coordinate and complex with multiple *ortho* phenolic hydroxyl of PCA to form a stable chelate,<sup>11,17</sup> which can improve the crosslinking degree of the system. PCA was self-assembled and deposited on the surface of the PS core particles to form a dark brown shell, which can absorb the influence of incoherent scattered light and increase the contrast of the photonic crystals.<sup>21,22</sup> The surface shell of polydopamine-coated polystyrene core-shell nanoparticles (PS@PDA NPs) was rough and had a certain thickness, which could thermal-assisted self-assemble amorphous photonic crystal structure and eliminate the iridescent effect. However, the fabrication of PS@PDA NPs was time consumed.

In this work, we proposed a method to prepare PS@PCA-Cu(II) core-shell microspheres and thermal-assisted self-assemble amorphous photonic crystals to fabricate non-angle-dependent structure colored cotton fabric.  $\text{Cu}^{2+}$  was used as an oxidant and  $\text{NaBO}_3 \cdot 4\text{H}_2\text{O}$  as a trigger to promote the rapid oxidative polymerization of CA, and PCA was coated on the surface of PS with good monodispersity to form PS@PCA-Cu(II) core-shell structure colloidal microspheres. The CA concentration,  $\text{NaBO}_3 \cdot 4\text{H}_2\text{O}$  concentration,  $\text{Cu}^{2+}$  concentration, reaction time and temperature were investigated to obtain the optimum preparation process. The surface morphology, color performance, fastness performance and anti-ultraviolet performance of structural colored cotton fabrics prepared with six different PS@PCA-Cu(II) particle sizes were characterized. The obtained structural color cotton fabric has soft and uniform color, no angle dependence, stable mechanical fastness and excellent anti-ultraviolet function. The preparation method has the advantages of simple operation, environmental friendliness and excellent performance, which provides a new idea for the preparation of structural color materials.

## 2 Experimental section

### 2.1 Materials

Cotton fabric (twill fabric,  $103 \text{ g m}^{-2}$ , warp density: 40 threads per cm; weft density: 22 threads per cm) was provided by

Jiangsu Shazhou Printing and Dyeing Group (China) and used after being washed with lye soap. Caffeic acid and sodium perborate tetrahydrate ( $\geq 97.0\%$  purity) was purchased by Shanghai Aladdin Bio-Chem Technology Co., LTD., China. Cupric chloride anhydrous was supplied by Shanghai Titan Scientific Co., Ltd., China. Polystyrene microspheres were bought from Nanjing China Biotechnology Co., Ltd. All the chemicals were of analytical reagent grade and used without further purification.

### 2.2 Preparation of PS@PCA-Cu(II) nanospheres triggered by $\text{CuCl}_2/\text{NaBO}_3 \cdot 4\text{H}_2\text{O}$

1 g PS dispersion (10 wt%) was dissolved in 50 mL HAC-NaAC buffer solution (pH 7), and ultrasonically dispersed for 30 minutes. CA ( $2 \text{ mmol L}^{-1}$ ),  $\text{NaBO}_3 \cdot 4\text{H}_2\text{O}$  ( $3 \text{ mmol L}^{-1}$ ) and  $\text{CuCl}_2$  ( $1 \text{ mmol L}^{-1}$ ) were added to the PS microsphere dispersion to obtain CA-Cu(II) modified PS nanoparticles. The magnetic stirring speed was 1400 rpm, and the reaction was carried out at  $50^\circ\text{C}$  for 10 min. The obtained PS@CA-Cu(II) microsphere dispersion was centrifuged to collect the PS@CA-Cu(II) precipitate, and the precipitate was diluted again to 5 wt% for preparation of the structural color film.

### 2.3 Self-assembled structure color film on white cotton fabric

Thermally assisted gravity deposition method was used to prepare structural color film. 5 mL PS@PCA-Cu(II) microsphere dispersion was added to a Petri dish (6 cm of diameter) containing a white cotton fabric sample. The Petri dish was placed in a  $50^\circ\text{C}$  oven until the solution was completely evaporated, and finally the prepared fabric was heated at  $80^\circ\text{C}$  for 2 h to ensure the latex spheres were tightly fixed on the fabric by caffeic acid (Fig. 1).

### 2.4 Characterization

The average hydrodynamic diameter and polydispersity index (PDI) of colloidal nanospheres were measured by Nano particle size analyzer (Nano-ZS90, Malvern, England). Red-green index (a) and blue-yellow index (b) are all determined by Hunter Lab Ultra Scan PRO reflectance spectrophotometer (Hitachi High Technologies America, Inc.; Schaumburg, IL, USA). D65 light source and  $10^\circ$  observation angles were used, and the coating surface was directed toward the light source. The average value was obtained after four tests. The total reflection spectrum was measured by an ARM-type micro-angle-resolving spectrometer (Shanghai Fuxiang Instrument Equipment Co., Ltd.), and the range of wavelength was 350–750 nm. The morphology of amorphous photonic structures (APS) on the cotton fabric was observed by a field emission scanning electron microscopy (FESEM, Hitachi S-4800, Japan) and a transmission electron microscopy (TEM, HT7700, Japan). The color fastness and washing resistance of structurally color fabric was examined by a sandpaper abrasion test and simulated washing test, respectively.<sup>23,24</sup> The UV protection factor (UPF) of the cotton fabric was measured using a Lab Sphere UV-1000F transmission analyzer (Lab sphere, Inc., North Sutton, VA USA). The average



Fig. 1 Preparation of biomimetic non-iridescent structural color based on polystyrene–polycaffeic acid core–shell nanospheres.

of four tests on a single layer fabric was taken as the measurement result.

### 3 Results and discussion

Aiming at the problem that the color of structural color materials turns white due to the presence of background light and uncorrelated scattered light, in this work,  $\text{Cu}^{2+}$  and  $\text{NaBO}_3 \cdot 4\text{H}_2\text{O}$  were added to promote the rapid oxidation and polymerization of CA. The dark brown film formed by complexed with  $\text{Cu}^{2+}$  was used as a black absorbent and coated PS to form core–shell colloidal microspheres PS@PCA- $\text{Cu}(\text{II})$ .<sup>17</sup> The effects of CA concentration, the concentration of  $\text{NaBO}_3 \cdot 4\text{H}_2\text{O}$  and  $\text{Cu}^{2+}$ , reaction temperature and time on the color rendering effect of the structural color were discussed below.

#### 3.1 The effect of CA concentration on structured color

When the PS particle size was 196 nm, the temperature was 50 °C, the reaction time was 10 min, the concentration ratio of  $\text{NaBO}_3 \cdot 4\text{H}_2\text{O}$  to CA was 9 : 2, and the concentration ratio of  $\text{Cu}^{2+}$  to CA was 2 : 1, the effect of CA concentrations on color rendering were discussed. The experimental results are shown in Fig. 2.

The dark brown PCA- $\text{Cu}(\text{II})$  film was used as a black absorber to coat the PS to eliminate the influence of incoherent light, so the dark brown film has a great influence on the color rendering effect. As shown in Fig. 2, when the CA concentration is 0.5 mmol  $\text{L}^{-1}$ , the amount of caffeic acid involved in oxidative polymerization and complexation is less, the ability to eliminate incoherent light interference is weak, and the structural color fabric shows grey color. When the CA concentration is greater than or equal to 4 mmol  $\text{L}^{-1}$ , the degree of polymerization of PCA is higher, and the color of the PCA- $\text{Cu}(\text{II})$  film is dark enough to cover the structural color of the three-dimensional photonic crystal structure. As shown in Fig. 2(d–f), the total reflection curve has no obvious reflection peak and the overall reflectivity is low, the optical image appears black, and the color rendering effect is poor. When the CA concentration is 1 mmol  $\text{L}^{-1}$  and 2 mmol  $\text{L}^{-1}$ , the color rendering effect is more suitable.

As shown in Fig. 2, when the CA concentration increases from 1 mmol  $\text{L}^{-1}$  to 2 mmol  $\text{L}^{-1}$ , the hue of the structural color changes from blue to green, and the reflection peak red shifts as the CA concentration increases, which conforms to the modified Bragg diffraction equation:<sup>25</sup>

$$m\lambda = 1.633Dn \quad (1)$$

where  $m$  and  $\lambda$  are the diffraction order and reflection wavelength, respectively. The  $D$  and  $n$  are the interparticle distance between neighboring particles and the refractive index, respectively.

It can be seen from the Bragg diffraction equation that when other factors remain unchanged, the structural color of the photonic crystal (that is, the wavelength of visible light reflected by the photonic crystal) is related to the particle size of the self-assembly structural unit (PS@PCA- $\text{Cu}^{2+}$  colloidal microspheres). As the particle size increases,  $\lambda_{\text{max}}$  increases, that is,

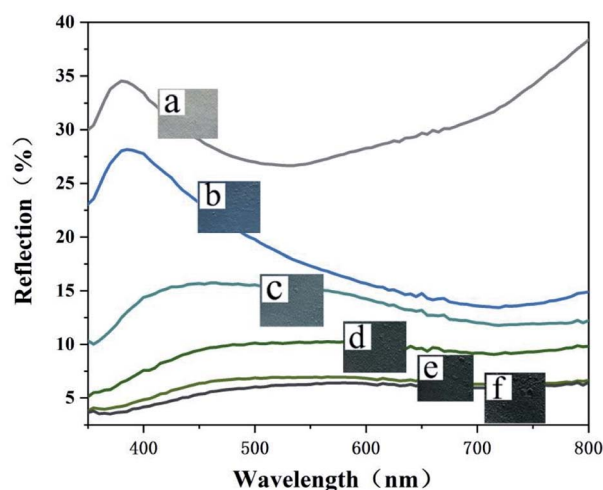


Fig. 2 The corresponding total reflectance spectra and images of structurally colored fabrics with different CA concentrations: CA: (a) 0.5 mmol  $\text{L}^{-1}$ , (b) 1 mmol  $\text{L}^{-1}$ , (c) 2 mmol  $\text{L}^{-1}$ , (d) 4 mmol  $\text{L}^{-1}$ , (e) 6 mmol  $\text{L}^{-1}$ , (f) 8 mmol  $\text{L}^{-1}$ .



the photonic band gap moves to the long-wave direction, and the structural color redshift occurs. Therefore, with the increase of CA concentration, the PCA coating layer becomes thicker, resulting in the increase of the particle size of PS@PCA-Cu(II) colloidal microspheres, the increase of  $\lambda_{\text{max}}$ , and the red shift of the structural color. When the concentration of CA increased from  $1 \text{ mmol L}^{-1}$  to  $2 \text{ mmol L}^{-1}$ , the hue changed from blue to green.

Theoretically, the structural hue of PS with same particle size can be changed within a certain range by controlling the CA concentration. However, in the actual reaction, the influence of incoherent light is difficult to eliminate when the CA concentration is low, and the fabric is whitened. When the CA concentration is higher, on one hand, the thickness of the coating layer increases, and the structural color red shifts further. On the other hand, the dark brown of the PCA coating layer is thick to cover the structural color, and the fabric appears black. Accordingly, it is not feasible to obtain the continuously variable structural hue by controlling the CA concentration, and only a suitable concentration of CA can be used to prepare the structural color.

In summary,  $1 \text{ mmol L}^{-1}$  and  $2 \text{ mmol L}^{-1}$  are the more appropriate dosages of CA when the PS particle size was  $196 \text{ nm}$ . Under these conditions, the next step of process was explored.

### 3.2 The influence of triggers on structural color

When the PS particle size was  $196 \text{ nm}$ , the temperature was  $50^\circ\text{C}$ , the reaction time was  $10 \text{ min}$ , the CA concentration was  $1 \text{ mmol L}^{-1}$  and  $2 \text{ mmol L}^{-1}$ , and the  $\text{Cu}^{2+}$  to CA concentration ratio is  $2:1$ , the influence of concentration ratios of  $\text{NaBO}_3 \cdot 4\text{H}_2\text{O}$  and CA on the structured color were discussed and the results are shown in Fig. 3 and 4.

The oxidation-reduction potentials of CA and  $\text{O}_2$  are very similar,<sup>26</sup> so the rate of oxidation and deposition of CA due to

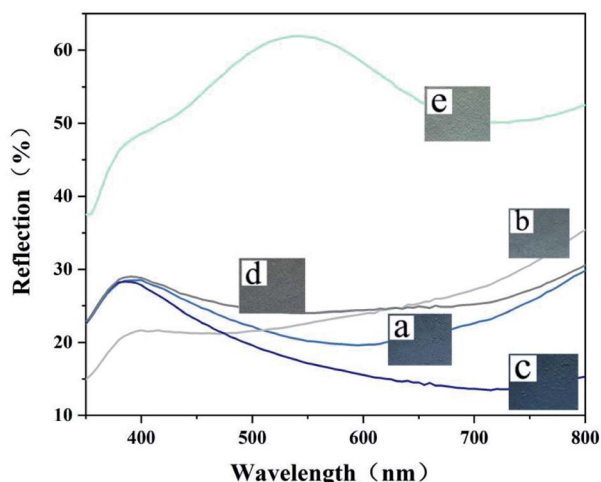


Fig. 3 The corresponding total reflectance spectra and images of structurally colored fabrics with different concentrations ratios of  $\text{NaBO}_3 \cdot 4\text{H}_2\text{O}$  and CA: the concentration of CA are  $1 \text{ mmol L}^{-1}$ , the concentration ratios of  $\text{NaBO}_3 \cdot 4\text{H}_2\text{O}$  and CA are (a)  $3:2$ , (b)  $6:2$ , (c)  $9:2$ , (d)  $12:2$ , (e)  $15:2$ .

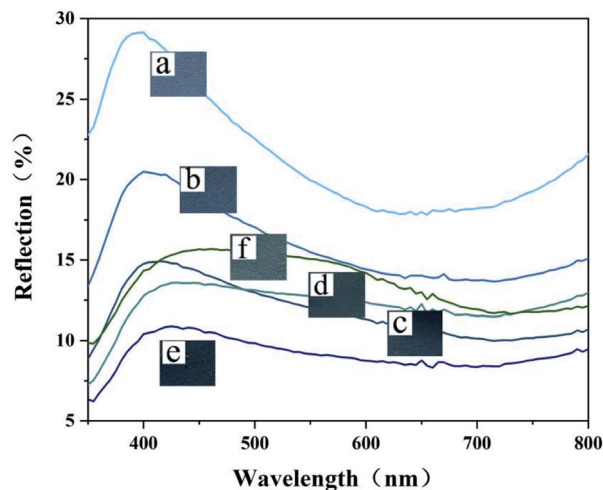


Fig. 4 The corresponding total reflectance spectra and images of structurally colored fabrics with different concentration ratios of  $\text{NaBO}_3 \cdot 4\text{H}_2\text{O}$  and CA (the concentration of CA are  $2 \text{ mmol L}^{-1}$ , the concentration ratios of  $\text{NaBO}_3 \cdot 4\text{H}_2\text{O}$  and CA are  $3:4$ ,  $6:4$ ,  $9:4$ ,  $12:4$ ,  $15:4$ ,  $18:4$ ).

dissolved oxygen in the air atmosphere is very slow. The research of Yang *et al.*<sup>17</sup> showed that no color change was observed after 12 hours of CA solution or  $\text{H}_2\text{O}_2/\text{CA}$  alone. However, the transparent yellow  $\text{CA}/\text{Cu}^{2+}$  solution slowly turned dark green after 12 hours in the air. While, the color of  $\text{CA}/\text{Cu}^{2+}$  solution with  $\text{Cu}^{2+}$  and dissolved oxygen as the oxidant and  $\text{H}_2\text{O}_2$  as the trigger quickly changed from transparent yellow to dark brown. This different phenomenon was attributed to the reactive oxygen species (ROS) formation from  $\text{H}_2\text{O}_2$  decomposition under  $\text{Cu}^{2+}$  oxidation, which induced the rapid semi-quinone conversion of CA monomers. Therefore, the performance and concentration of the triggering agent have a great influence on the color rendering effect of structural color.

In this work,  $\text{NaBO}_3 \cdot 4\text{H}_2\text{O}$  was chosen as the triggering agent instead of  $\text{H}_2\text{O}_2$  because  $\text{NaBO}_3 \cdot 4\text{H}_2\text{O}$  is unstable and can slowly release  $\text{H}_2\text{O}_2$  when dissolved in water (the sodium perborate anion ring structure is shown in Fig. 5).  $\text{NaBO}_3 \cdot 4\text{H}_2\text{O}$  can replace  $\text{H}_2\text{O}_2$  to play the oxidation role and make the caffeic acid uniformly polymerize, and prepare PCA-Cu(II) coating with moderate thickness and good uniformity. Meanwhile, it can overcome the shortcomings of hydrogen peroxide, such as poor stability, explosiveness, high toxicity, complicated operation and high cost.<sup>19,20,27</sup>

Based on the structural color change trend of the fabric in Fig. 3 and 4, when the concentration ratio of  $\text{NaBO}_3 \cdot 4\text{H}_2\text{O}$  to CA increases, the fabric gradually darkens so that no structural

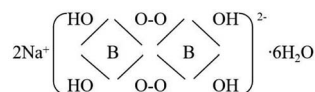


Fig. 5 Structure of sodium perborate tetrahydrate.





color can be observed. However, when  $\text{NaBO}_3 \cdot 4\text{H}_2\text{O}$  increases to excess, the reflectance curve shifts upward and the maximum reflection peak wavelength increases, the fabric turns white and the structural color occurs red shift (Fig. 3(e) and 4(f)), which is related to the oxidation mechanism of  $\text{NaBO}_3 \cdot 4\text{H}_2\text{O}$ . When the concentration ratio of  $\text{NaBO}_3 \cdot 4\text{H}_2\text{O}$  to CA is relatively low, as the ratio increases, the degree of PCA polymerization increases, the PCA coating layer becomes thicker, the PS@PCA particle size increases, so the reflectance curve shifts downward and the structural color red shifts; as the concentration of  $\text{NaBO}_3 \cdot 4\text{H}_2\text{O}$  increases, a large number of phenol groups are oxidized to a quinone structure, which reduces the proportion of hydroxyl groups chelated with  $\text{Cu}^{2+}$  in PCA, and the color of PS@PCA microspheres becomes lighter, which makes the color of the fabric white and cause waste of reagents. Fig. 4 fully reflects the phenomenon of disordered structural color change when  $\text{NaBO}_3 \cdot 4\text{H}_2\text{O}$  is relatively excessive. The concentration ratio of  $\text{NaBO}_3 \cdot 4\text{H}_2\text{O}$  and CA should be controlled to prevent excess. Therefore, from the perspective of resource saving and color rendering effect,  $2 \text{ mmol L}^{-1}$  CA and  $3 \text{ mmol L}^{-1}$   $\text{NaBO}_3 \cdot 4\text{H}_2\text{O}$  should be selected for the next process exploration.

### 3.3 Influence of $\text{CuCl}_2$ concentration on structured color

When the PS particle size was 235 nm, the temperature was  $50^\circ\text{C}$ , the reaction time is 10 min, the CA concentration was  $2 \text{ mmol L}^{-1}$ , and the  $\text{NaBO}_3 \cdot 4\text{H}_2\text{O}$  to CA concentration ratio was 3 : 2, the influence of different  $\text{Cu}^{2+}$  concentration on the structured color was investigated, and the results are shown in Fig. 6.

The introduction of  $\text{Cu}^{2+}$  has three main functions: first, it can be used as an oxidant to promote the self-polymerization of CA; second, it can promote the decomposition of  $\text{H}_2\text{O}_2$ , so that the decomposition of  $\text{NaBO}_3 \cdot 4\text{H}_2\text{O}$  into  $\text{H}_2\text{O}_2$  moves in the positive direction, enhancing the oxidation ability and improving the degree of polymerization of PCA; thirdly, it can

form a coordination complex with PCA and coat PS,<sup>17</sup> which absorbs the influence of incoherent scattered light in the structural color. Therefore, the concentration ratio of  $\text{Cu}^{2+}$  and CA has a great influence on the color rendering effect of the structural color.

As shown in Fig. 6, when the concentration ratio of  $\text{Cu}^{2+}$  to CA is 1 : 4, less  $\text{Cu}^{2+}$  is oxidized and complexed with PCA, and the fabric is white. When the concentration ratio of  $\text{Cu}^{2+}$  to CA is greater than or equal to 0.5, it is enough to present a soft structural color, and the reflectivity curve changes little with the increase of  $\text{Cu}^{2+}$  dosage. Accordingly, the concentration ratio with narrower half-peak width, bright color, and the least amount of metal ions was selected for the next process exploration, that is, the concentration ratio of  $\text{Cu}^{2+}$  to CA was 1 : 2,  $2 \text{ mmol L}^{-1}$  CA and  $1 \text{ mmol L}^{-1}$   $\text{Cu}^{2+}$ .

### 3.4 The effect of reaction temperature on structural color

When the PS particle size was 235 nm, the reaction time was 10 min, the CA concentration was  $2 \text{ mmol L}^{-1}$ , the  $\text{NaBO}_3 \cdot 4\text{H}_2\text{O}$  to CA concentration ratio was 3 : 2, the  $\text{Cu}^{2+}$  to CA concentration ratio was 1 : 2, the influence of different reaction temperature on the structured color was discussed and the experimental results are shown in Fig. 7.

Temperature has certain effects in the reaction system of  $\text{NaBO}_3 \cdot 4\text{H}_2\text{O}$  decomposition to  $\text{H}_2\text{O}_2$ , CA oxidative polymerization of PCA, the formation of dark brown coordinated complex with PCA and  $\text{Cu}^{2+}$  and coating of PS microspheres. The higher the temperature, the higher the reaction activity, and the greater the degree of response.

As shown in Fig. 7, under a temperature range of  $30^\circ\text{C}$  to  $80^\circ\text{C}$  and keeping other reaction conditions constant, the reflectance curve of the obtained structural color fabric is approximately a linear change. From the perspective of energy saving and color rendering effect,  $50^\circ\text{C}$  was chosen as the optimum reaction temperature, with which the narrowest

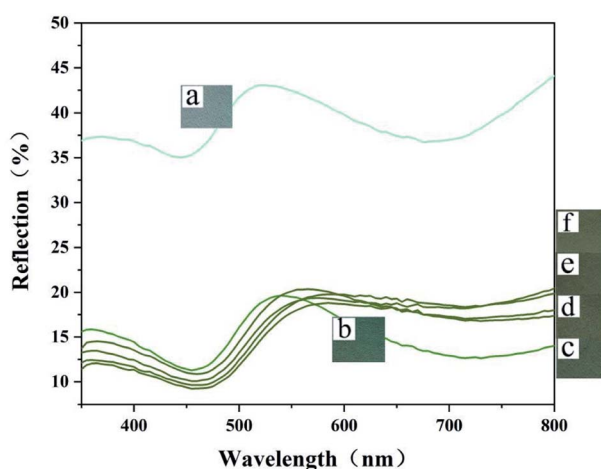


Fig. 6 The corresponding total reflectance spectra and images of structurally colored fabrics with different concentration ratios of  $\text{Cu}^{2+}$  and CA (the concentration of CA are  $2 \text{ mmol L}^{-1}$ , the concentration ratios of  $\text{Cu}^{2+}$  and CA are respectively 1 : 4, 1 : 2, 1 : 1, 2 : 1, 3 : 1, 4 : 1).

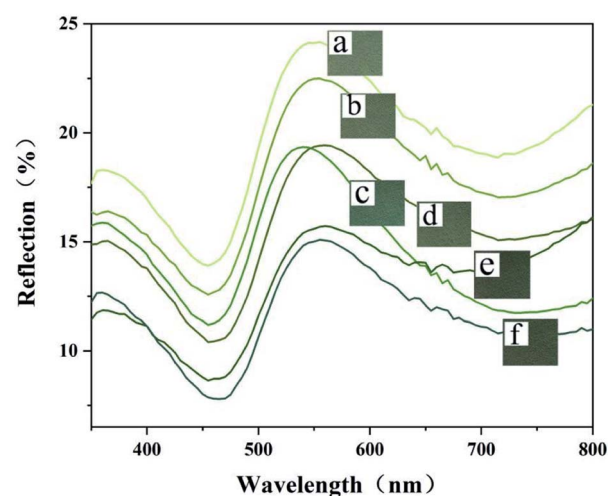


Fig. 7 The corresponding total reflectance spectra and images of structurally colored fabrics reacted at  $30^\circ\text{C}$ ,  $40^\circ\text{C}$ ,  $50^\circ\text{C}$ ,  $60^\circ\text{C}$ ,  $70^\circ\text{C}$  and  $80^\circ\text{C}$ .



reflection peak, the most suitable reflectivity, and the most vivid color of fabric can be achieved.

### 3.5 The effect of reaction time on structural color

When the PS particle size was 235 nm, the reaction time was 10 min, the CA concentration was  $2 \text{ mmol L}^{-1}$ , the  $\text{NaBO}_3 \cdot 4\text{H}_2\text{O}$  to CA concentration ratio was 3 : 2, the  $\text{Cu}^{2+}$  to CA concentration ratio was 1 : 2, the influence of different reaction temperature on the structured color were investigated. The experimental results are shown in Fig. 8.

As shown in Fig. 8, when the reaction time is less than or equal to 5 min, the degree of polymerization of PCA is low and the color of fabric is light because the reaction time is too short and the reaction is incomplete, leading to weak adhesion and insufficient coat ability to PS. Consequently, the ability to absorb incoherent scattered light and ambient light is weak, the fabric is white, and the coating is uneven. When the reaction time is greater than or equal to 10 minutes, the reaction is sufficient and uniform structural color fabric can be obtained. With the increase of reaction time, the color of the PCA- $\text{Cu}^{2+}$  shell becomes darker, thus covering the structural color and decreasing the reflection. From the perspective of color vividness and energy saving, 10 min was chosen as the optimum reaction time.

### 3.6 Structured colored fabrics with different PS particle diameters and their color performance

Fig. 9 shows the images of the structurally colored cotton fabric coated with six different particle size PS microspheres under the optimum conditions: the reaction temperature is  $50^\circ\text{C}$ , the reaction time is 10 minutes, the CA concentration is  $2 \text{ mmol L}^{-1}$ , the  $\text{NaBO}_3 \cdot 4\text{H}_2\text{O}$  and CA concentration ratio is 3 : 2, and the  $\text{Cu}^{2+}$  and CA concentration ratio is 1 : 2. Combining the optical picture of Fig. 9 and the color measurement data in Fig. 10, it can be known that this process effectively eliminates

the influence of incoherent scattered light and ambient light accompanying the color development of the amorphous photonic crystal structure. The PS@PCA- $\text{Cu}(\text{II})$  modified cotton fabric presents soft and uniform structural color.

### 3.7 Morphologies of as-prepared PS@PCA- $\text{Cu}(\text{II})$

In this work, thermally assisted gravity deposition method was used to prepare structural color film.<sup>19,20</sup> When the fabric was immersed in the PS@PCA- $\text{Cu}(\text{II})$  emulsion, the gravity of the particles dispersed in the solvent was greater than the buoyancy in the water, and the particles spontaneously accumulate on the fabric at the bottom of the solution. At the same time, during the process of colloid assembly, the evaporation of the edge of the emulsion was the fastest, so that the water carried the PS@PCA- $\text{Cu}(\text{II})$  colloidal microspheres to the edge of the emulsion. Due to the entropy of the system, the colloidal microspheres assembled into an ordered structure at the fabric-emulsion-air contact line. As the liquid evaporated, the microspheres moved with the contact line, and finally a large-area ordered colloidal array was obtained.

Generally, photonic crystals utilize PS, polymethyl methacrylate (PMMA) and  $\text{SiO}_2$  microspheres to produce structural color. The microspheres have a smooth surface (Fig. 11(a<sub>1</sub>)). Under the action of system entropy, they assemble regular and long-range orderly periodic arrangements as shown in Fig. 11(a<sub>2</sub>). The structure of this periodic arrangement is anisotropic, and the color produced can change with the viewing angle, which limits the application of structural colors in the color field. The surface of the caffeic acid-modified colloidal microspheres is rough (as shown in Fig. 11(b<sub>1</sub>) and 11(b<sub>2</sub>)), the surface roughness of these particles prevented the generation of colloidal crystal structures,<sup>18</sup> resulting in the formation of short-range ordered and long-range disordered amorphous photonic crystal structures. This is a special defect state structure with isotropy, which greatly reduces the angle dependence of the structural color, so that the structural color does not change with the angle. Fig. 12 shows the structural color cotton fabric observed at  $0^\circ$ ,  $30^\circ$  and  $60^\circ$  angles, which proves that the self-assembled amorphous photonic crystal structure of PS microspheres modified by PCA can effectively eliminate the angle dependence of the structural color.

### 3.8 Fastness of structurally colored cotton fabric

The stability of the assembled physical structures on fabrics were evaluated by the simulated washing test and the sandpaper rubbing test, which was usually used as the common test methods for color fastness of textiles.

It can be seen from Fig. 13, in the simulated washing test, under the conditions of  $50^\circ\text{C}$  and 60 rpm, part of the PS@PCA coating falls off the surface of cotton fabric, the transmittance of the washing residue decreases to a certain extent, but the layer is still relatively complete and has a certain washing fastness. As shown in Fig. 14, the rubbing fastness test of sandpaper demonstrates that the coating structure is damaged to a certain extent after 30 times rubbing with a 50 g weight, and the structural color can still be observed.

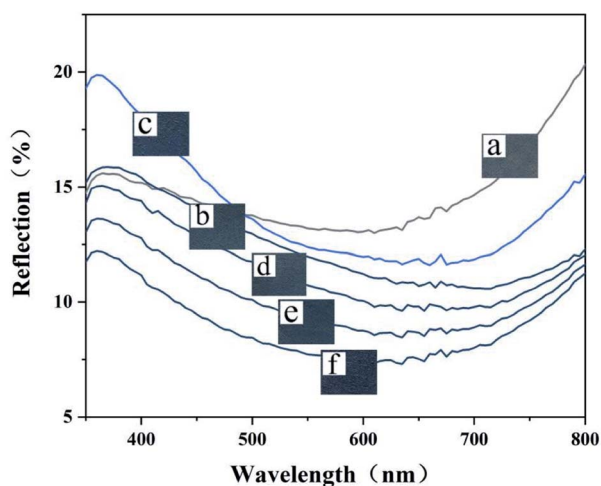


Fig. 8 The corresponding total reflectance spectra and images of structurally colored fabrics with reaction time of 3 min, 5 min, 10 min, 15 min, 20 min and 25 min.



Fig. 9 (a–f) Images of the structurally colored fabric coated with PS@PCA–Cu(II) NPs, the diameters of PS NPs are 196 nm (blue), 210 nm (green), 235 nm (yellow-green), 260 nm (pink), 297 nm (Fuchsia), 306 nm (purple).

### 3.9 UV resistance of PS@PCA–Cu(II) modified cotton fabric

With the awareness of the harmfulness of excessive ultraviolet exposure, people's requirements for the UV resistant textiles are gradually increasing. Common photonic crystal structure color fabrics prepared by PS, polymethylmethacrylate (PMMA) and silica microspheres have the problem of lack of surface functional groups. The UV transmittance curves of the cotton samples and UV Protection Factor (UPF) results are shown in Table 1. Compared with the untreated cotton fabric, the transmittance of PS@PCA-coated cotton fabric is greatly reduced, and the average UPF value is 44.74. The result shows that PS@PCA-coated cotton fabrics has good UV resistance.

### 3.10 Advantages and disadvantages of PS@PCA–Cu(II) modified cotton fabric

The cost issue greatly limits the application of traditional PS@PDA modified cotton fabrics, while the natural plant polyphenol CA has lower cost and anti-UV function, which improves the possibility of product application and increases its added value. At the same time, the amorphous photonic crystal structure eliminates the angle dependence and has wider application in the field of display materials. Admittedly, the

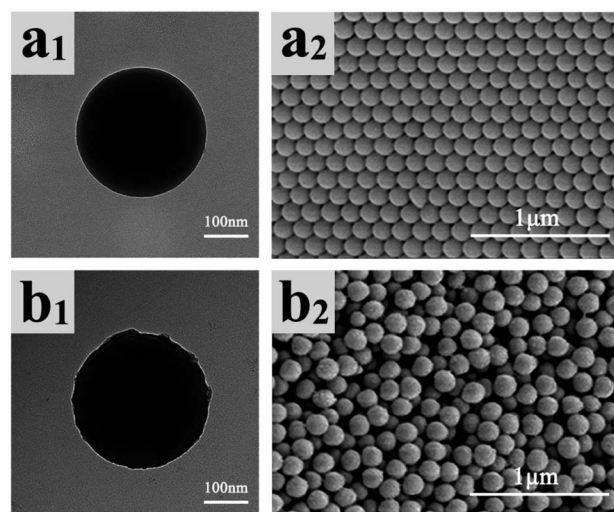


Fig. 11 TEM image of (a<sub>1</sub>) PS and (b<sub>1</sub>) PS@PCA–Cu(II) NPs; top-view SEM images of (a<sub>2</sub>) PS and (b<sub>2</sub>) PS@PCA–Cu(II) photonic coatings on CF; the mean size of PS@PCA–Cu(II) NPs is 306 nm.

process also has certain limitations. The PS@PCA structural color fabric has soft and uniform color, and the dark shell can effectively absorb the interference of incoherent scattered light,

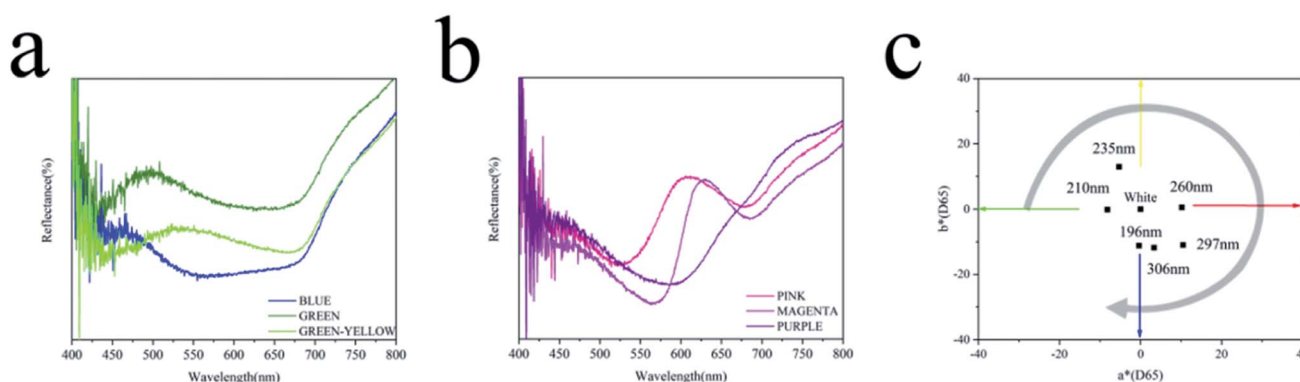


Fig. 10 (a) Reflection spectra of the blue, green and green-yellow colored films on CF, (b) reflection spectra of the pink, magenta and purple colored films on CF, (c) CIE 1931 chromaticity coordinates of PS@PCA–Cu(II) coating on CF with various color.







Fig. 12 Optical image of the magenta colored films on CF at different view angles.

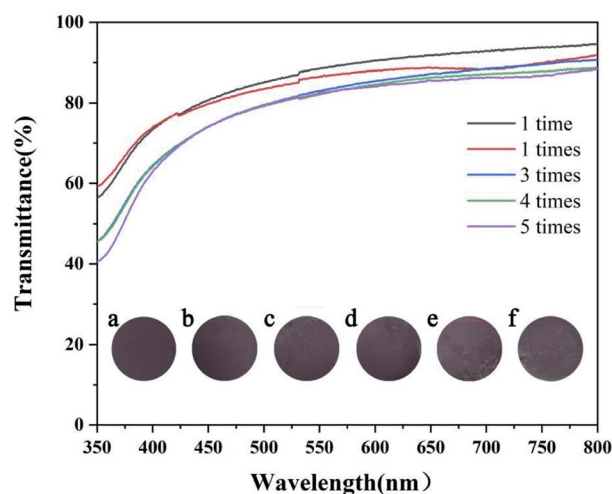


Fig. 13 The transmittance of the washing liquid; optical images of (a) unwashed fabric sample and (b–f) five fabric samples after different washing cycle.

however, the color is not very vivid due to its amorphous photonic crystal structure. Although the structural stability of amorphous photonic crystals has been improved to some extent, it is still far from practical application.

Table 1 UPF of cotton fabric samples

Samples	Transmittance (%)		UPF
	UVA	UVB	
Untreated	29.11	25.83	3.75
PS@PCA-coated	2.28	2.26	44.74

## 4 Conclusions

A reasonable preparation method of PS@PCA-Cu(II) nano-spheres to generate structural color was established. The optimum preparation process was obtained as follows: 1 mmol  $\text{L}^{-1}$   $\text{CuCl}_2$ , 3 mmol  $\text{L}^{-1}$   $\text{NaBO}_3 \cdot 4\text{H}_2\text{O}$ , 2 mmol  $\text{L}^{-1}$  CA, 2 g  $\text{L}^{-1}$  PS are reacted at 50 °C for 10 minutes, the PS@PCA-Cu(II) nano-spheres were prepared by rapid oxidation polymerization of CA and coated with PS and self-assembled amorphous photonic crystal structure through thermal-assisted gravity sedimentation. The structural color cotton fabric with soft and uniform color, no angle dependence, stable mechanical fastness and excellent UV resistance was prepared. The preparation method has the advantages of simple operation, short time-consuming and environmental friendliness, which provides a novel idea for the preparation of structural color materials.

## Author contributions

Tianchen Wei: conceptualization, methodology, investigation, writing – original draft, visualization. Xiaowei Zhu: conceptualization, methodology, investigation. Xueni Hou and Yijiang Li: data curation, instrument appointment and testing. Aoqing Dong, Xinying Jiang and Yu Huang: investigation, data curation. Tieling Xing: conceptualization, methodology, writing – review & editing, supervision, project administration. Xue Dong, Xiangrong Wang and Guoqiang Chen: supervision, writing – review & editing.

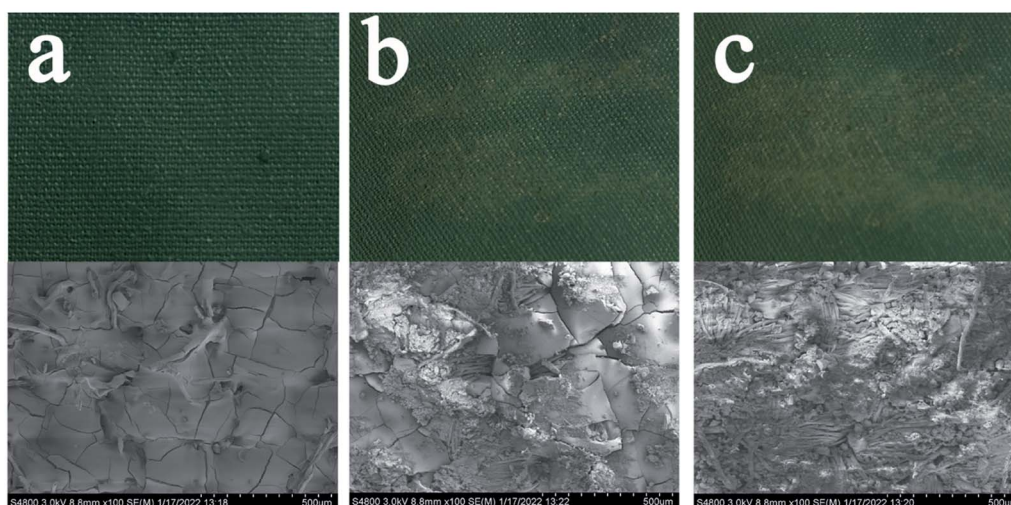


Fig. 14 Optical images and top-view SEM images of PS@PCA coating on CF (a) before, (b) after 15 and (c) 30 times rubbing.





## Conflicts of interest

There are no conflicts to declare.

## Acknowledgements

This work was supported by National Natural Science Foundation of China (51973144, 51741301); Postgraduate Research & Practice Innovation Program of Jiangsu Province (KYCX21-2960); the National Undergraduate Training Program for Innovation and Entrepreneurship, China (202010285045, 202010285036Z).

## References

- 1 S. Kinoshita, S. Yoshioka, Y. Fujii and N. Okamoto, Photophysics of structural color in the Morpho butterflies, *Forma*, 2002, **17**(2), 103–121.
- 2 J. P. Ge, J. Goebl, L. He, Z. D. Lu and Y. D. Yin, Rewritable photonic paper with hygroscopic salt solution as ink, *Adv. Mater.*, 2009, **21**, 4259–4264.
- 3 J. D. Joannopoulos, S. G. Johnson, J. N. Winn and R. D. Meade, Photonic crystals: molding the flow of light, *Comput. Sci. Eng.*, 1995, **3**, 38–47.
- 4 O. Meskini, A. Abdelghani, A. Tlili, R. Mgaith, N. Jaffrezic-Renault and C. Martelet, Porous silicon as functionalized material for immunosensor application, *Talanta*, 2007, **71**, 1430–1433.
- 5 F. Villa, J. A. Gaspar-Armenta and F. Ramos-Mendieta, One-dimensional photonic crystals: equivalent systems to single layers with a classical oscillator like dielectric function, *Opt. Commun.*, 2003, **216**(4–6), 361–367.
- 6 A. Huttunen and P. Torma, Band structures for nonlinear photonic crystals, *J. Appl. Phys.*, 2002, **91**(7), 3988–3991.
- 7 S. H. Kim, Y. L. Su, S. M. Yang and G. R. Yi, Self-assembled colloidal structures for photonics, *NPG Asia Mater.*, 2011, **3**(1), 25–33.
- 8 C. T. Chen, J. Pedrini, E. A. Gauding, C. Kastl, G. Calafiore, S. Dhuey, T. R. Kuykendall, S. Cabrini, F. M. Toma and S. Aloni, Very high refractive index transition metal dichalcogenide photonic conformal coatings by conversion of ALD metal oxides, *Sci. Rep.*, 2019, **9**(1), 214.
- 9 Y. Liu, J. Hu and Z. H. Wu, Fabrication of coatings with structural color on a wood surface, *Coatings*, 2020, **10**(1), 32.
- 10 J. D. Simon and D. N. Peles, The Red and the Black, *Acc. Chem. Res.*, 2010, **43**(11), 1452–1460.
- 11 T. S. Sileika, D. G. Barrett, R. Zhang, K. H. A. Lau and P. B. Messersmith, Colorless Multifunctional Coatings Inspired by Polyphenols Found in Tea, Chocolate, and Wine, *Angew. Chem., Int. Ed.*, 2013, **52**, 10766–10770.
- 12 W. Z. Qiu, Q. Z. Zhong, Y. Du, Y. Lv and Z. K. Xu, Enzyme-Triggered Coatings of Tea Catechins/Chitosan for Nanofiltration Membranes with High Performance, *Green Chem.*, 2016, **18**, 6205–6208.
- 13 F. J. You, Y. C. Xu, X. B. Yang, Y. Q. Zhang and L. Shao, Bio-inspired Ni<sup>2+</sup>-Polyphenol Hydrophilic Network to Achieve Unconventional High-Flux Nanofiltration Membranes for Environmental Remediation, *Chem. Commun.*, 2017, **53**, 6128–6131.
- 14 M. Ignatova, N. Manolova, I. Rashkov and N. Markova, Quaternized chitosan/kappa-carrageenan/cafeic acid-coated poly(3-hydroxybutyrate) fibrous materials: Preparation, antibacterial and antioxidant activity, *Int. J. Pharm.*, 2016, **513**(1–2), 528–537.
- 15 A. Saija, A. Tomaino, R. L. Cascio, D. Trombetta, A. Progettente, A. D. Pasquale, N. Uccella and F. Bonina, Ferulic and caffeic acids as potential protective agents against photooxidative skin damage, *J. Sci. Food Agric.*, 1999, **79**(3), 476–480.
- 16 D. G. Barrett, T. S. Sileik and P. B. Messersmith, Molecular diversity in phenolic and polyphenolic precursors of tannin-inspired nanocoatings, *Chem. Commun.*, 2014, **50**, 7265–7268.
- 17 Y. He, Q. Chen, Y. J. Zhang, Y. P. Zhao and L. Chen, H<sub>2</sub>O<sub>2</sub>-Triggered Rapid Deposition of Poly(caffeic acid) Coatings: A Mechanism-Based Entry to Versatile and High-Efficient Molecular Separation, *ACS Appl. Mater. Interfaces*, 2020, **12**(46), 52104–52115.
- 18 A. Kawamura, M. Kohri, G. Morimoto, Y. Nannichi, T. Taniguchi and K. Kishikawa, Full-Color Biomimetic Photonic Materials with Iridescent and Non-Iridescent Structural Colors, *Sci. Rep.*, 2016, **6**, 33984.
- 19 J. M. Matthews, Bleaching with Sodium Perborate, *J. Ind. Eng. Chem.*, 1911, **3**(3), 191–193.
- 20 L. K. Huang and G. Sun, Durable and Oxygen Bleach Rechargeable Antimicrobial Cellulose: Sodium Perborate as an Activating and Recharging Agent, *Ind. Eng. Chem. Res.*, 2003, **42**(22), 5417–5422.
- 21 B. Yi and H. F. Shen, Facile fabrication of crack-free photonic crystals with enhanced color contrast and low angle dependence, *J. Mater. Chem. C*, 2017, **5**, 8194–8200.
- 22 F. H. Li, B. T. Tang, S. L. Wu and S. F. Zhang, Facile Synthesis of Monodispersed Polysulfide Spheres for Building Structural Colors with High Color Visibility and Broad Viewing Angle, *Small*, 2017, **13**(3), 1602565.
- 23 Y. C. Li, L. Q. Chai, X. H. Wang, L. Zhou, Q. G. Fan and J. Z. shao, Facile Fabrication of Amorphous Photonic Structures with Non-Iridescent and Highly-Stable Structural Color on Textile Substrates, *Materials*, 2018, **11**(12), 2500.
- 24 Y. Meng, B. T. Tang, B. Z. Ju, S. L. Wu and S. F. Zhang, Multiple colors output on voile through 3D colloidal crystals with robust mechanical properties, *ACS Appl. Mater. Interfaces*, 2017, **9**(3), 3024–3029.
- 25 B. Li, C. Ouyang, D. P. Yang, Y. M. Ye, D. K. Ma, L. Luo and S. M. Huang, Noniridescent structural color from enhanced electromagnetic resonances of particle aggregations and its applications for reconfigurable patterns, *J. Colloid Interface Sci.*, 2021, **604**, 178–187.
- 26 J. C. Danilewicz, Mechanism of Autoxidation of Polyphenols and Participation of Sulfite in Wine: Key Role of Iron, *Am. J. Enol. Vitic.*, 2011, **62**, 319–328.
- 27 K. Kurin-Csörgei, E. Poros-Tarcali, I. Molnar, M. Orban and I. Szalai, Chemical Oscillations With Sodium Perborate as Oxidant, *Front. Chem.*, 2020, **8**, 561788.

